

Contrail coverage derived from 2001 AVHRR data over the continental United States of America and surrounding areas

RABINDRA PALIKONDA¹, PATRICK MINNIS*², DAVID P. DUDA³ and HERMANN MANNSTEIN⁴

¹Analytical Sciences and Materials, Inc., Hampton, Virginia, USA

²Science Directorate, NASA Langley Research Center, Hampton, Virginia, USA

³Hampton University, Hampton, Virginia, USA

⁴DLR Institut für Physik der Atmosphäre, Oberpfaffenhofen, Wessling, Germany

(Manuscript received March 23, 2004; in revised form October 18, 2004; accepted March 29, 2005)

Abstract

Linear contrail coverage, optical depth, and longwave radiative forcing are derived from NOAA-15 and NOAA-16 Advanced Very High Resolution Radiometer data taken during daytime over the continental United States of America (USA), southern Canada, northern Mexico, and the adjacent oceans. Analyses were performed for all available overpasses during 2001, but for NOAA-15 were primarily limited to the eastern half and the northwestern corner of the domain. Contrail coverage averaged 1.17 % and 0.65 % from the early morning NOAA-15 and midafternoon NOAA-16, respectively, for the areas and month common to both satellites. The NOAA-16 contrail coverage and radiative properties for the limited NOAA-15 domain are, on average, nearly identical to those for the entire domain. The estimated combined maximum coverage for the entire domain was ~ 1.05 % during February, while the minimum of 0.57 % occurred during August. Mean optical depths varied by ~ 20 % with winter minima and summer maxima. The annual mean optical depth of 0.27 translated to a normalized contrail longwave radiative forcing of 15.5 Wm^{-2} . The overall daytime longwave radiative forcing for the domain is 0.11 Wm^{-2} . The normalized radiative forcing peaked during summer while the overall forcing was at a maximum during winter because of the greater contrail coverage. A detailed error analysis showed that the linear contrail coverage was overestimated by ~ 40 % for both satellites the true coverage is closer to 0.70 and 0.40 % for NOAA-15 and 16, respectively. Errors in the mean NOAA-15 optical depths and radiative forcing were negligible while their NOAA-16 counterparts were overestimated by approximately 13 %. Contrail coverage was dramatically lower than expected from previous studies, but is most likely due to the significant decrease in upper tropospheric humidity observed in numerical weather analysis data. Contrail optical depths are much greater than both theoretical estimates for this part of North America and empirical retrievals over Europe. The cause of the morning-afternoon difference in contrail coverage is not yet known. Further modelling studies and additional satellite analyses are needed to understand this diurnal cycle and to explain the differences between the present and previous results.

Zusammenfassung

Der Bedeckungsgrad an linearen Kondensstreifen, deren optische Dicke und der daraus resultierende Strahlungsantrieb werden aus NOAA-15 und NOAA-16 Advanced Very High Resolution Radiometer Daten über den Vereinigten Staaten von Nordamerika (USA), dem südlichen Kanada, nördlichem Mexiko und den angrenzenden Meeresgebieten abgeleitet. Die Analysen wurden für alle vorhandenen Tagpassagen im Jahr 2001 durchgeführt, wobei aber NOAA-15 auf die Osthälfte und den nordwestlichen Teil des Gebietes beschränkt war. Als Bedeckungsgrad wurde für die morgendlichen NOAA-15 Daten 1,17 % und nachmittags für NOAA-16 0,65 % für die übereinstimmenden Gebiete und Zeiten gefunden. Der Bedeckungsgrad und die optischen Eigenschaften für das Gesamtgebiet stimmen bei NOAA-16 mit denen des begrenzten NOAA-15 Gebietes überein. Der höchste Bedeckungsgrad war ~ 1.05 % im Februar, das Minimum im August mit 0,57 %. Die optische Dicke variierte um 20 % zwischen dem Winterminimum und dem Sommermaximum. Der jährliche Mittelwert von 0,27 führt zu einem langwelligen Strahlungsantrieb von $15,5 \text{ Wm}^{-2}$. Im Mittel über das Gesamtgebiet beträgt der langwellige Strahlungsantrieb $0,11 \text{ Wm}^{-2}$. Der normalisierte Strahlungsantrieb hat sein Maximum im Sommer, während der Gesamtstrahlungsantrieb wegen des höheren Bedeckungsgrades ein winterliches Maximum hat. Eine ausführliche Fehleranalyse zeigt, dass der Kondensstreifenbedeckungsgrad bei beiden Satelliten um ~ 40 % für beide überschätzt wurde, so dass der wahre Bedeckungsgrad eher bei 0,70 % für NOAA-15 und 0,40 % für NOAA-16 liegt. Fehler in der optischen Dicke und im Strahlungsantrieb sind bei NOAA-15 unerheblich, während sie bei NOAA-16 um etwa 13 % überschätzt wurden. Der Kondensstreifenbedeckungsgrad war drastisch niedriger als aus früheren Untersuchungen erwartet. Mit hoher Wahrscheinlichkeit ist dies jedoch eine Folge der deutlich verringerten Feuchtigkeit der oberen Troposphäre. Die hier bestimmte optische Dicke ist höher als theoretische Schätzungen für die USA erwarten lassen und auch höher als die über Europa bestimmten Werte. Die Ursachen für den Unterschied zwischen Vor- und Nachmittag sind noch unbekannt. Weitere Modellstudien und zusätzliche Satellitenanalysen sind erforderlich, um den Tagesgang und die Unterschiede zwischen den gegenwärtigen Ergebnissen und früheren Studien zu erklären.

1 Introduction

Contrails often lead to the development of additional cirrus clouds that can affect climate via the radiation budget. Evaluation of contrail coverage and optical properties is crucial for assessing the impact of current and future climatic effects of air traffic. Current estimates of contrail coverage over the United States of America (USA) and surrounding areas have been based on a single NOAA-16 (N16) afternoon overpass time for recent studies and at four times of day for 1993–94 data from two satellites with different sensitivities and detection errors (PALIKONDA et al., 1999). Approximately 25,000 flights cross portions of the USA each day at different times of day. The commercial flight activity begins in earnest around 0600 LT and continues at relatively constant high intensity prior to fading shortly before local midnight (GARBER et al., 2005). Because spreading contrail life-times are generally less than 4–6 hours (DUDA et al., 2001; MINNIS et al., 2002), the atmosphere should be cleansed of most contrail coverage by the beginning of the next day. If it is assumed that the state of the upper troposphere is, on average, the same during the day, this daily cycle should be reflected in the contrail properties and coverage. Given the air traffic diurnal cycle, the amount of contrail coverage detected during morning satellite overpasses should be the same as that from data taken during the afternoon. However, if a given air mass is penetrated by a large number of flights over the course of the day, it is possible that the contrail coverage during the afternoon would be less than during the morning because the spreading and saturation of contrails formed earlier in the day might mask contrails formed during the afternoon or decrease the amount of available moisture such that contrail growth is stymied during the afternoon. To obtain a better assessment of the average contrail coverage and its diurnal variation over this part of the world, this study analyzes data taken during 2001 from NOAA-15 (N15) in the early morning and from N16 during the afternoon. This time period was selected to facilitate comparison with and adjustments to model estimates of contrail coverage based on recently available high-resolution numerical weather analyses (DUDA et al., 2005). The results constitute the beginning of a much longer-term climatology of contrails over a significant portion of North America.

2 Data and methodology

The satellite data used for this study consist of 1-km radiances from the morning (~0730 LT) N15 and

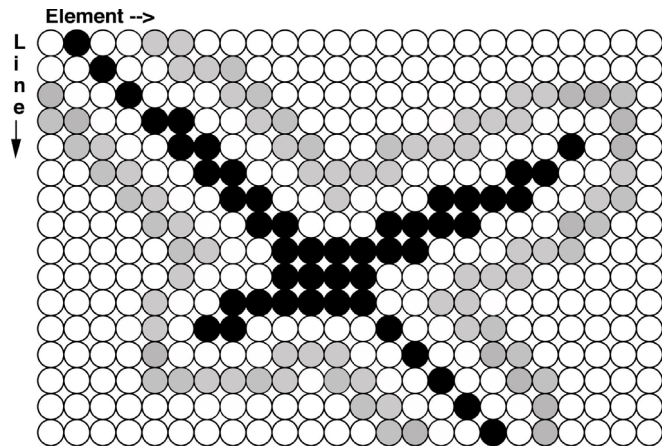


Figure 1: Schematic of pixels used for computing background radiances. Black – contrail; Gray – background; white – unused.

mid-afternoon (~1430 LT) N16 Advanced Very High Resolution Radiometer (AVHRR) passes over the parts of North America, Atlantic Ocean, and Pacific Ocean within the area between 25°N and 55°N and 65°W and 130°W. This domain is divided into a 30 x 65 1°-region grid. Images from all available overpasses are analyzed to calculate the contrail statistics, however, only data taken at viewing zenith angles less than 50° are used because contrail coverage tends to increase when data from greater viewing angles are considered (PALIKONDA et al., 1999). Monthly mean maps of the statistics are computed using only those regions having more than 90 % of the expected number of pixels during a given overpass and having at least ten images each month. Domain averages are computed using all available pixels.

The N16 data were analyzed first. Unfortunately, the Monterey, California N15 AVHRR receiving station failed during July 2000 and did not resume regular service until April 2002. This failure resulted in the loss of many western regions for the analyses. N15 data for the northwestern-most part of the domain were obtained from the Gilmore Creek, Alaska receiving station. In addition, many of the N15 overpasses for January and October 2001 at other stations yielded corrupted data and are not included in the results. N15 data that include the entire western portion of the domain will be analyzed later as the development of the contrail climatology continues.

The contrail mask used to classify a pixel as contrail or otherwise is the image processing algorithm of MANNSTEIN et al. (1999), which exploits the linear structure of contrails and the emissivity difference between 10.8 and 12.0 μm for fresh contrails compared to natural cirrus. The smaller ice crystals in young contrails cause a larger difference between the AVHRR channels 4 (10.8 μm) and 5 (12.0 μm) brightness temperatures (e.g., MINNIS et al., 1998a) than is found for natural cirrus clouds, which generally have larger ice crystals.

*Corresponding author: Patrick Minnis, MS 420, NASA Langley Research Center, Hampton, VA, 23681, USA, e-mail: p.minnis@nasa.gov

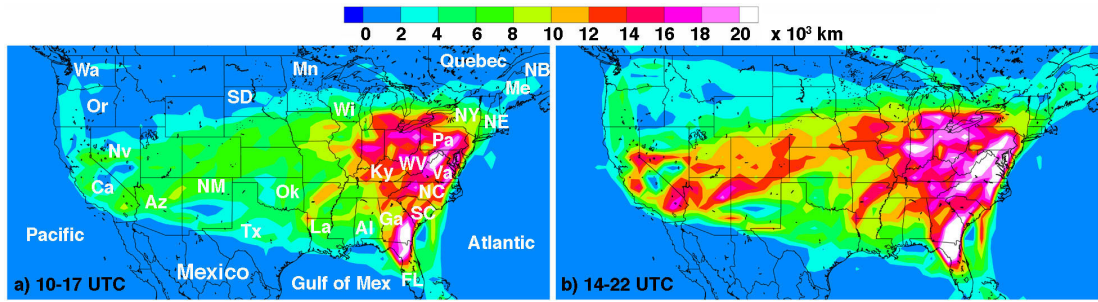


Figure 2: Annual mean air traffic in cumulative km travelled above 7 km per 1° region for (a) N15 overpass times and (b) N16 overpass times. Abbreviations correspond to states discussed in the text.

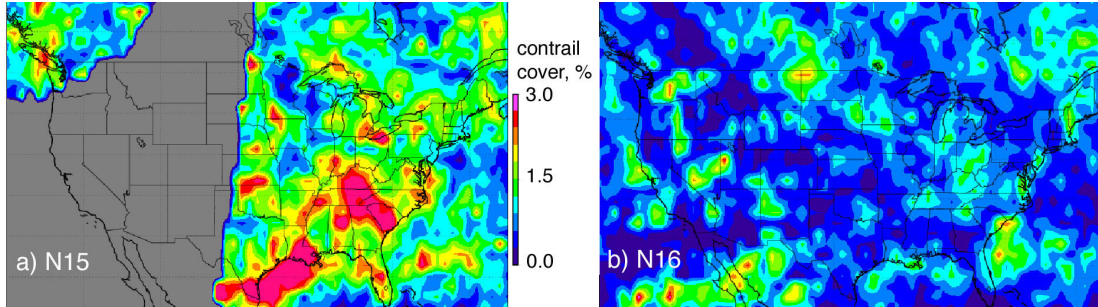


Figure 3: April 2001 daytime contrail coverage.

The algorithm works on the normalized 12- μm temperature and 10.8 μm –12 μm brightness temperature difference (BTD) images. The normalized images are passed through a line filter at multiple orientations and pixels are flagged as contrails if they satisfy certain temperature thresholds and geometric features. This technique primarily detects younger contrails because older contrails tend to lose some of their linearity and their particle sizes increase (MINNIS et al., 1998b; DUDA et al., 2001) resulting in a smaller BTD signal.

The fractional contrail areal coverage f_c for each image is simply the number of contrail pixels divided by the total number of pixels within the domain between 25°N and 55°N and 65°W and 130°W. After contrail pixels are identified, the visible optical depth, and contrail longwave radiative forcing CLRF are computed in following steps.

Assuming a typical contrail temperature of $T_{con} = 224\text{K}$ (MEYER et al., 2002), the contrail emissivity for a given pixel with an 10.8- μm temperature T_4 is

$$\varepsilon = \frac{\{B(T_4) - B(T_b)\}}{\{B(T_{con}) - B(T_b)\}} \quad (2.1)$$

where B is the Planck function at 10.8- μm and the background temperature T_b is computed from surrounding non-contrail pixels. The background radiance is calculated as the average radiance of all pixels at a distance of 2 pixels horizontally, vertically, or diagonally from a contrail pixel that are not adjacent to any other contrail pixels. The background pixels for a hypothetical pair of crossing contrails are shaded gray in Fig. 1. To en-

sure that the background pixels are below the contrail, $T_b > T_u$. Otherwise, T_b is invalid. If no pixels meeting these criteria are found, the mean background radiance, calculated for all other contrail pixels within the local 10' grid box, is used.

The visible optical depth τ for the contrails is derived from the emissivity using the parameterization of MINNIS et al. (1993),

$$\varepsilon = 1 - \exp[a(/\mu)b] \quad (2.2)$$

which accounts for the infrared scattering. In (2.2), μ is the cosine of the viewing zenith angle, and the coefficients, $a = -0.458$ and $b = 1.033$, are for an axisymmetrical 20- μm hexagonal ice column. To minimize false detections, all contrails with $\tau > 1$ were eliminated from the processing. The contrail longwave (LW; 5–50 μm) radiative forcing CLRF is defined as

$$CLRF = (Q_b - Q_c)f_c, \quad (2.3)$$

where Q_c and Q_b are the LW fluxes for contrails and the background respectively. Broadband LW fluxes are calculated from the 10.8- μm radiances as described by MINNIS and SMITH (1998). The normalized CLRF, NCLRF, is simply the difference, $Q_b - Q_c$.

Figure 2 shows the annual mean air traffic flown above 7 km over a large portion of the domain as computed from the database of GARBER et al. (2005) for the times that envelope all of the N15 (Fig. 2a) and N16 (Fig. 2b) overpass times for the entire domain. The plot shows the cumulative length of all flights within a given

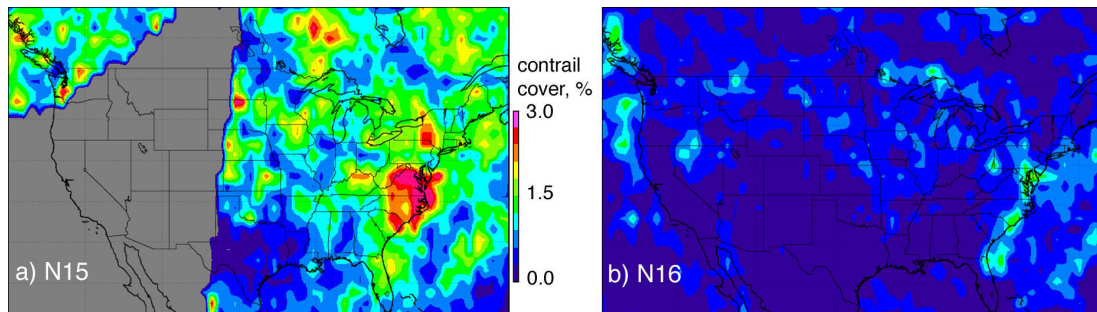


Figure 4: July 2001 daytime contrail coverage

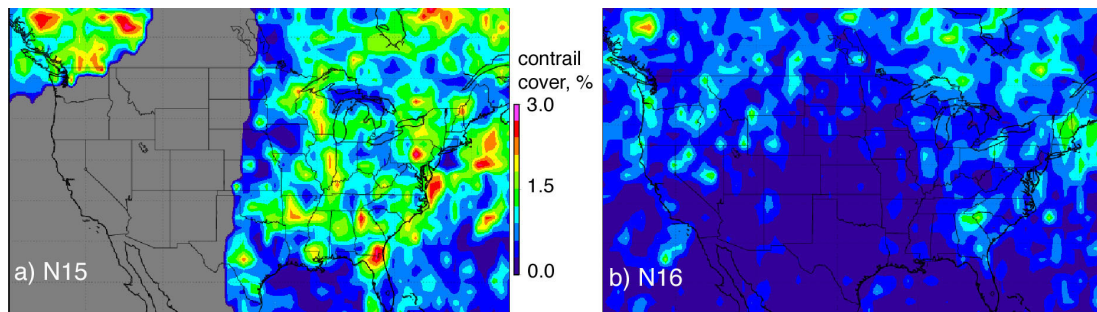


Figure 5: September 2001 daytime contrail coverage.

$1^\circ \times 1^\circ$ latitude-longitude region for those hours. Also shown in Fig. 2a are the geographical locations of selected states and provinces for reference in later discussion. Air traffic is heavier during the afternoon than during the morning at all locations despite the inclusion of 1 less hour during the afternoon.

3 Results

Figures 3–6 show the monthly distribution of contrail cover over the domain. During April, for the morning overpass (N15, Fig. 3a), maximum contrail coverage occurs over the southeastern states, off the coasts of Texas (Tx in Fig. 2) and Louisiana (La), and in northern Ohio (above WV). In the afternoon (N16, Fig. 3b), maximum coverage occurs over North Dakota (above SD), Nevada (NV), Washington (Wa), northern Mexico, and adjacent Pacific Ocean, areas not available from N15. The N15 maximum over the western Gulf of Mexico is still evident as a relative maximum in the N16 results. The domain averages are 1.29 % and 0.71 % in the morning and afternoon, respectively. These means include differing numbers of regions. The morning July contrail cover (Fig. 4a) peaks over Virginia, North Carolina (NC), South Carolina (SC), and New York (NY). Minimum coverage occurs over Texas (Tx), Louisiana, Alabama (Al), and Minnesota (MN). The areal coverage is almost 70 % less during the afternoon (Fig. 4b). A local maximum occurred along the Atlantic coast from Virginia to Florida (FL), and off the coasts of Oregon (Or), Washington, and British Columbia (north of Wa). These areas

of maximum coverage are similar to those in the N15 retrievals. The substantial morning-afternoon difference in areal coverage persists in September (Fig. 5). During the morning (Fig. 5a), maximum contrail coverage exceeds 2 % over southwestern Canada, Georgia (Ga), Pennsylvania (Pa), and east of Virginia. The extensive contrail minimum in the afternoon (Fig. 5b) is defined by a triangle extending from southern California (Ca) to South Dakota (SD) and to the tip of Florida. Maximum coverage occurred over British Columbia (north of Wa), Oregon, New England (NE), and Quebec. During the winter, in the morning (Fig. 6a), contrail cover exceeds 1.5 % over the southeastern states and Gulf of Mexico, and off the coast of Oregon and Washington. The afternoon coverage during December (Fig. 6b) peaks over northern Virginia, West Virginia, and Pennsylvania. Local maxima are seen over New Mexico (NM), Wisconsin (Wi), and west of California.

When averaged over all 12 months, the distributions produce more distinct patterns (Fig. 7). The contrail coverage is concentrated over the eastern third of the domain during the morning (Fig. 7a) with maxima over Lake Erie, New York, Kentucky (Ky), Virginia, the Carolinas (NC and SC), and Florida. Relative maxima are also apparent over southern and northern portions of Canada with a relative minimum in between them. In addition to having less contrail coverage than seen in the morning, the pattern during the afternoon (Fig. 7b) is different. The relative maxima over the eastern part of the domain occur off the coast of Florida and over New Jersey and Pennsylvania. Over the central USA, fewer contrails occur over Oklahoma (Ok) while more are ob-

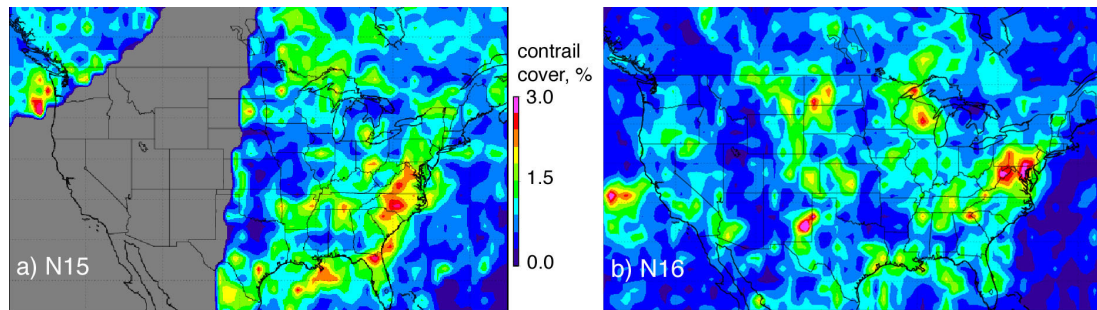


Figure 6: December 2001 daytime contrail coverage.

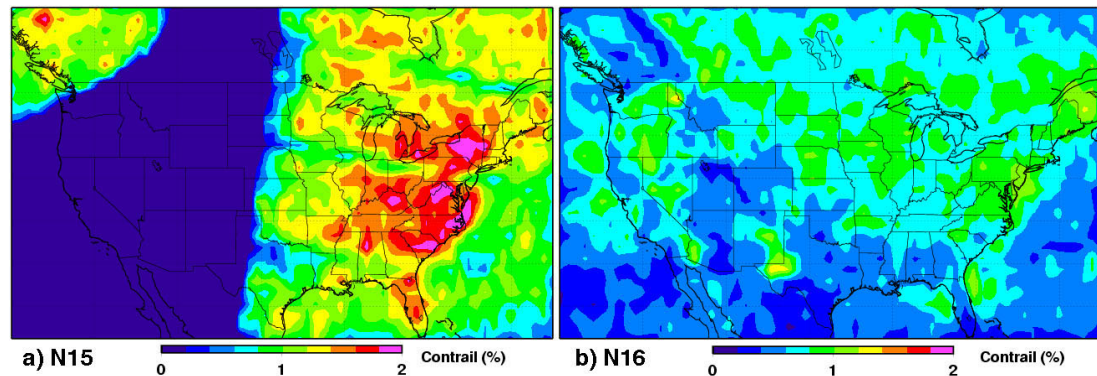


Figure 7: Mean 2001 daytime contrail coverage over USA domain.

served to the north. Over many areas, relative minima that are observed in the morning are replaced with relative maxima during the afternoon and vice versa. Maxima are also evident over Washington, Oregon, southwestern Arizona (Az), and southeastern New Mexico (NM), areas not observed with N15. A pronounced minimum occurs over the central Rocky Mountains. Relative maxima are also seen off the California coast and, during the morning and afternoon, east of Maine (Me) over New Brunswick (NB), Canada.

The seasonal variations in contrail coverage from both satellites are summarized in Table 1. The results include the monthly means from each satellite for the limited domain sampled by N15 as well as the monthly average for the two satellites. Contrail coverage during the afternoon (i.e., N16) peaks during the winter and is at a minimum during July, differing by a factor of 3 (Table 1) and is nearly same in both phase and magnitude for the entire and limited domains. However, as expected from Figs. 3–7, the contrail coverage during the morning is nearly twice that observed in the afternoon and the seasonal cycle is much less apparent. The coverage in the morning over the N15 domain is at a maximum during May and at a minimum during August and September with a range of 0.46 %. This range is less than the afternoon seasonal variation in both absolute and relative terms. The most variation between morning and afternoon is seen during the summer months when the contrail coverage differs by a factor of 2 to 3.

Considering only the eastern half of the domain, on average, the combined contrail coverage ranges from a minimum of 0.71 % during August to a maximum of 1.07 % in February. Between February and May, the mean varies by only 0.10 %. Similarly, between July and September, it varies by only 0.03 %. Thus, the periods of minima and maxima are broad and the actual extrema at a given time of day or in a given year could occur in months other than February and August. Given that the N16 mean for the limited domain in Table 1 is nearly identical to that for the entire domain, the ratios of the combined limited domain values to the N16 values were multiplied by the N16 values of f_c for the entire domain to estimate the combined coverage for the entire domain. The missing N15 months were filled via linear interpolation. The results in the last column of Table 1 show the broad winter-spring maximum with a seasonal range of 0.48 %.

The mean values for OD, CLR, and NCLRF are summarized in Table 2 for the limited and entire domains for N15 and N16, respectively. The results for N16 over the N15 limited domain were not substantially different from those for the entire domain and are, therefore, not included. The mean contrail optical depths in Table 2 vary seasonally to some degree. The summer maxima are 20–30 % greater than the February minima. The annual mean optical depths, computed with contrail coverage weighting, from N16 are 0.28 compared to 0.26 from N15. This 12 % difference is relatively consistent from month to month. The N15 and

Table 1: Contrail coverage (%) during 2001 for N15 and N16 for limited domain (see Fig. 3a) and for N16 and estimated combined N15 and N16 total domain.

Month	limited domain			total domain	
	N15	N16	combined	N16	estimated combined
January	—	—	—	0.92	1.03
February	1.19	0.95	1.07	0.93	1.05
March	1.16	0.91	1.03	0.86	0.97
April	1.31	0.69	1.00	0.71	1.03
May	1.40	0.54	0.97	0.55	0.99
June	1.22	0.43	0.83	0.44	0.85
July	0.94	0.37	0.75	0.33	0.67
August	0.94	0.47	0.71	0.38	0.57
September	0.96	0.49	0.73	0.45	0.67
October	—	—	—	0.71	0.90
November	1.04	0.81	0.93	0.84	0.97
December	0.97	0.79	0.88	0.80	0.89
Annual	1.17	0.65	0.88	0.66	0.88

Table 2: N-16 contrail radiative properties for entire domain and N15 contrail properties for limited domain, 2001.

Month	N16	N16	N16	N15	N15
	OD	CLRF (Wm^{-2})	NCLRF (Wm^{-2})	OD	NCLRF (Wm^{-2})
January	0.25	0.10	11.4	—	—
February	0.24	0.10	10.7	0.23	11.4
March	0.26	0.11	12.3	0.24	11.6
April	0.28	0.12	16.7	0.25	14.3
May	0.31	0.11	20.1	0.27	16.6
June	0.30	0.09	19.7	0.26	16.8
July	0.31	0.07	21.3	0.28	18.0
August	0.30	0.08	21.8	0.27	18.9
September	0.30	0.09	19.8	0.28	17.0
October	0.31	0.14	19.3	—	—
November	0.28	0.13	15.7	0.26	13.8
December	0.28	0.11	14.2	0.26	13.1
Annual	0.28	0.11	15.8	0.26	15.1

N16 monthly frequency distributions of contrail optical depth in Figure 8 are remarkably consistent. During all months, $0.2 < OD < 0.4$ for more than 30 % of the contrails. Thicker contrails were observed more frequently in summer than during the winter and spring.

The contrail radiative forcing (Table 2) in the morning was greatest during the summer months and at a minimum during February. In the afternoon, the maximum and minimum CLRF occurred during October and July, respectively. CLRF depends on both the contrail coverage and its background. The monthly mean NCLRF varies smoothly through the seasons for both satellites. In the morning, NCLRF varies from 11 Wm^{-2} in February to 19 Wm^{-2} during August. During the afternoon, NCLRF varies from 11 Wm^{-2} in March to 22 Wm^{-2} during August indicating that the thermal contrast changed by more than a factor of 2 between winter and summer during the afternoon for the entire domain. The f_c -weighted annual mean values are very similar, together averaging 15.4 Wm^{-2} .

4 Discussion

4.1 Error analysis

The differences in contrail coverage between the two satellites may be due, in part, to different sensitivities of channels 4 and 5 on the two AVHRRs. Each channel has a slightly different spectral response function and slightly different calibration. Small differences in each channel can translate to large differences in the BTD relative to the pixel-use threshold value. Visually, the BTD images from the two satellites are quite different when constructed using the same temperature range and contrast suggesting that the contrail retrievals would be different using the same methodology. Some insight into those differences might be gained by examining the errors for the two satellites. The automated detection method (MANNSTEIN et al., 1999) is based on BTD values that produce a linear feature in the image. This assumption of linearity can cause both under- and over-estimates of contrail coverage. Contrails do not always maintain linearity causing the technique to miss some of them. Natural clouds, rivers, and coastlines can also produce linear features that can be mistaken as contrails. Additionally, some contrails can be missed because their signals are insufficient to be detected. The technique is also sensitive to background variations and to minor peculiarities in the relative calibrations of the AVHRR channels 4 and 5. Thus, it is essential to estimate the errors in the detection method for each satellite and region analyzed. PALIKONDA et al. (1999) roughly estimated that the error rate for applying the same methodology to AVHRR data from NOAA-11 and 12 resulted in a 25 % overestimate of the contrail coverage for the same domain. MEYER et al. (2002) developed more rigorous correction methods (e.g., false alarm rate, stationary artifacts, detection efficiency) for their NOAA-14 AVHRR contrail analysis over Europe.

Here, a user-interactive computer program was applied in the same manner as described by MINNIS et al. (2005) to evaluate the results for each satellite using 3 randomly selected days during 3 different months. In the program, the pixels identified as contrails are overlaid on the T4 and BTD images. The results are examined both objectively by comparing T4 and BTD values for the contrails with the surroundings and subjectively using contrast adjustment. Contrail pixels can be added or deleted based on the analyst's judgment. Results are stored as images with each pixel identified as non-contrail or remaining, deleted, or added contrail. The contrail properties are then computed for all three of the latter categories.

Table 3 summarizes the error analyses for the selected days for each month and satellite. In general, for these days, f_c appears to be overestimated by ~ 40 %. For N16, the deleted fraction accounts for roughly 57 %

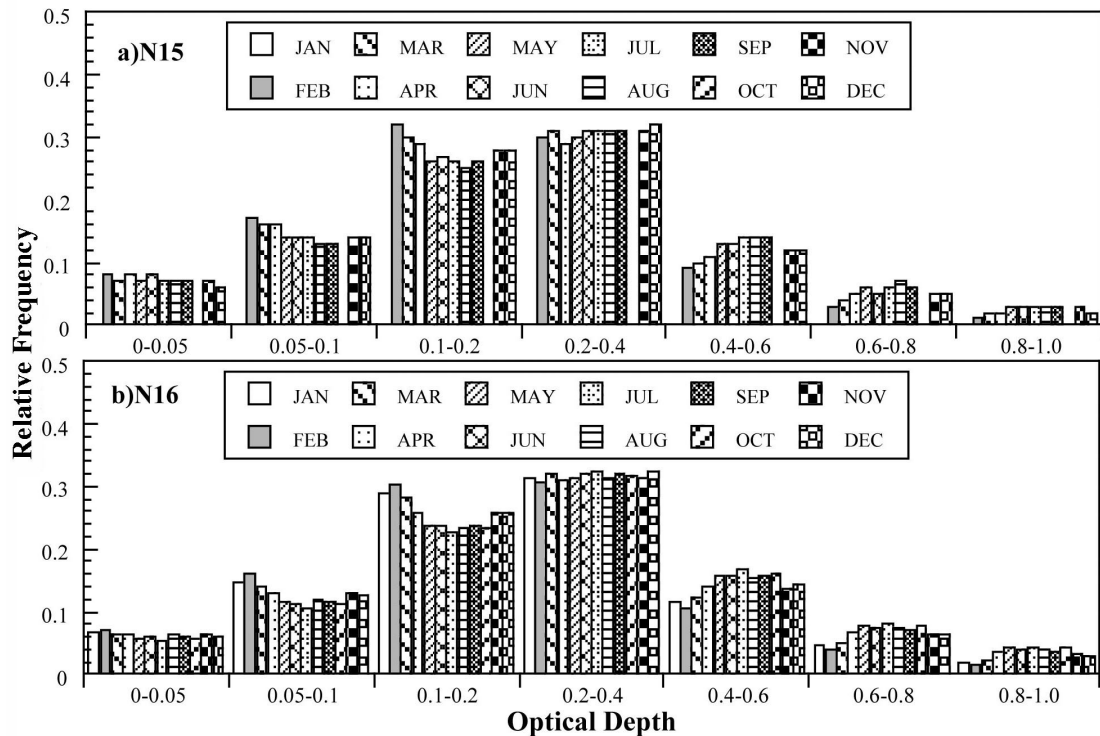


Figure 8: Histogram of daytime contrail optical depths from NOAA-15 and NOAA-16 over USA, 2001.

Table 3: Contrail error analysis results for 3 randomly selected days during each month in 2001. Correction factor (CF) is unitless.

	Contrail Coverage (%)			Optical Depth			NCLRF (Wm^{-2})		
	remain	del/add	CF	remain	del/add	CF	remain	del/add	CF
N15									
April	0.70	0.55/0.08	0.62	0.31	0.23/0.25	1.10	16.6	12.2/13.1	1.10
July	0.57	0.55/0.12	0.62	0.26	0.28/0.16	0.90	18.5	17.8/11.6	0.95
December	0.56	0.42/0.02	0.59	0.28	0.25/0.17	1.03	13.8	11.2/8.2	1.07
mean	0.57	0.48/0.07	0.61	0.28	0.25/0.19	1.01	16.2	14.0/11.7	1.03
N16									
Feb	0.52	0.49/0.05	0.56	0.20	0.19/0.13	0.99	11.8	8.4/6.9	1.12
April	0.32	0.54/0.18	0.58	0.27	0.30/0.18	0.82	17.3	19.5/10.8	0.90
July	0.15	0.21/0.05	0.56	0.25	0.32/0.17	0.79	18.8	22.7/11.7	0.81
mean	0.31	0.41/0.10	0.57	0.24	0.27/0.17	0.87	14.8	16.5/10.4	0.87

of the original contrail coverage compared to 46% for N15. The fraction added is slightly larger for N16 but is only about 25 % of the deleted amount. To quantify the overall impact of the error a correction factor, $CF(f_c)$, was computed by dividing the remaining and added contrails by the original contrail fraction. The value of $CF(f_c)$ is remarkably consistent from one month to the next averaging 0.61 and 0.57 for N15 and N16, respectively. Thus, the true linear contrail coverage is likely to be 40 % less than the values in Table 1. As indicated in Figure 9, however, the greatest reductions in contrail coverage were outside the USA boundaries in areas of light air traffic. These sizeable negative errors can explain the unexpectedly large values of f_c in Canada north of $50^\circ N$. It is likely that the overestimate of contrail coverage within the continental USA is less than the 40 % average for the entire domain. The 40 % overestimate

for the current results is slightly greater than that reported by MINNIS et al. (2005) who applied the same error analysis to N16 data over an ocean background confirming that surface variability adds to false detections.

To estimate the random component of the error, standard deviations of the differences between the original and corrected images were computed for each region. Based on a maximum of 9 images, the mean regional standard deviations are 1.21 and 1.36 % coverage for N15 and N16, respectively, or 103 % and 209 % in a relative sense. These rather large errors are dominated by the false detections over Canada and the occurrence of cirrus streaks around the edges of large-scale cyclones or deep convective systems. Assuming that these results are representative and accounting for the bias errors, the relative standard errors in the monthly mean for a given

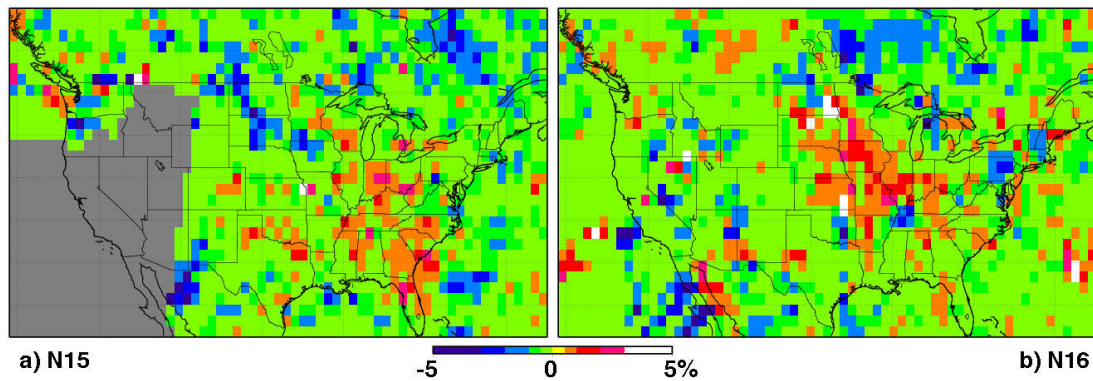


Figure 9: Change in contrail coverage after errors analysis for 9 randomly selected days as described in the text.

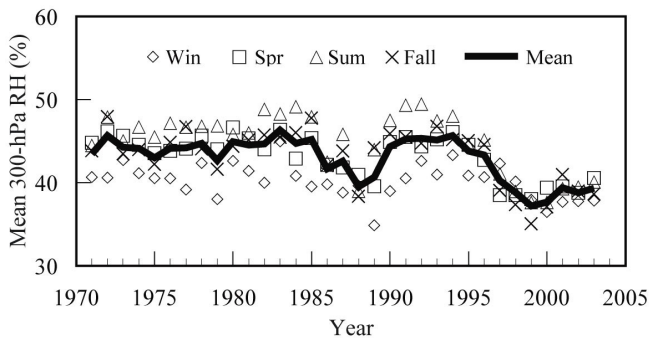


Figure 10: Seasonal and annual mean NCEP RH at 300 hPa over USA.

region are 18 % and 38 % for N15 and N16, respectively. These errors are not geographically uniform; some areas will have much larger or smaller errors in the monthly mean. As the averaging area increases, the uncertainty in the regional mean decreases. Random errors in the domain monthly means in an absolute sense are less than 0.01 % for each satellite. Thus, the morning-afternoon differences on the domain scale are statistically significant.

Errors were also examined using only those pixels with viewing zenith angles exceeding 50° . At those higher viewing angles, 60–70 % of the contrail pixels were false detections while roughly 10 % were added. The net result is similar to the analysis of MEYER et al. (2002) who showed a doubling of the false alarm rate at high angles. It is also consistent with the viewing zenith angle dependence of contrail coverage reported by PALIKONDA et al. (1999).

On average, the contrail optical depths for N15 are nearly identical for the original and corrected contrail coverage. The optical depths for the remaining N16 contrails, however, are 11 % smaller than the deleted mean value. In all cases, the added contrails are thinner, in the mean, than the original contrails. Overall, there appears to be no need to correct the N15 optical depths, while the N16 ODs should probably be reduced by ~ 13 %. Similar correction factors were found for NCLRF. The contrail properties for the selected days appear to be repre-

sentative of the entire dataset. In all cases, τ and NCLRF are typically within less than 10 % of their counterparts in Table 2. The correction factors indicate that the N16 OD and NCLRF values in Table 2 should be equal to or slightly less, instead of being larger, than the N15 values.

The error analysis was conducted without the optical depth restriction. For N15, 1.1 % of the remaining and added contrails had $OD > 1$ compared to 0.4 % of the deleted pixels. Only 0.4 % of the N16 remaining and added contrails had $OD > 1$, while 0.6 % of the deleted pixels were optically thick. Thus, the exclusion of $OD > 1$ in the generation of the statistics had little impact on the results.

4.2 Comparison with air traffic patterns

The distribution of contrail coverage should be related in some fashion to the density of air traffic. At least for areas south of 50°N , the respective (a) and (b) panels in Figs. 2 and 7 can serve as a basis for examining that relationship. In a general sense, the contrail coverage in Fig. 7a over the eastern half of the domain is larger over areas with greater air traffic. For example, f_c tails off as the air traffic decreases to the west of Kentucky. It also decreases northward from southern Quebec before increasing again in areas with large errors (Fig. 9) and is much smaller over the Atlantic than over most other parts of the sampled domain. On a more detailed level, the maxima and minima from the two datasets are not in one-to-one correspondence. The air traffic lane over coastal Virginia and North Carolina (Fig. 2a), for example, appears to have a relative minimum in f_c while the maximum is shifted eastward by 100–200 km (Fig. 7a). Similarly, the air traffic maximum over southeastern Georgia and northeastern Florida does not yield a relative f_c maximum in the same area; it appears to be shifted entirely into Florida. Such traffic-contrail dislocations are common and are due to several effects such as contrail advection and the location of the saturated humidity field relative to the air traffic. DUDA et al.

(2001) provide some dramatic examples of the former effect, while the latter effect is discussed in section 5.

Similar shifts are evident in the N16 results but the general correspondence between air traffic density and f_c is not as clear as seen for the N15 results. Maximum contrail coverage is no longer concentrated over the eastern USA. The peak regional values are near the Texas border with New Mexico near a relative maximum in air traffic. The north-south air corridor in central California crossing the east-west corridor through central Nevada is reflected in the contrail coverage. Air traffic through western Washington and Oregon and southern California apparently results in relative maxima in f_c 100–200 km to the east. The relative minima over other heavily travelled parts of the western half of the domain are most likely due to a combination of unfavorable temperature and humidities at flight altitudes and the local circulation effects induced by the mountainous terrain.

4.3 Diurnal variation

The error analysis indicates that the contrail mask works essentially the same for both satellites. Enhancement of the N16 BTM and T4 imagery during the error analyses did not reveal any significantly obvious new contrails, relative to N15, that were not detected with the automated algorithm. The added fractional coverage was about the same for both. However, there remains some possibility that there is a lower detection efficiency, even visually, during the afternoon over land when the surface is hot and the background heterogeneity is increased. Despite this potential, the OD distributions in Fig. 8 are essentially the same so that the retrieval for one satellite is not systematically missing thinner or thicker contrails relative to the other satellite retrieval. Thus, it appears that the morning-afternoon difference in coverage is not an artifact of the analyses, but, rather, a real phenomenon. MINNIS et al. (2003) found that contrail frequency observed from the surface over the USA peaked around 0800 LT (close to N15 overpass time) and was $\sim 25\%$ less around 1430 LT (the N16 overpass time). Although the relative difference in frequency observed from the surface is only half of that in coverage (Table 1), the two changes both indicate a morning-to-afternoon decrease in contrails. These differences occur despite the air traffic maximum extending from 0900 to 1600 LT (GARBER et al., 2005) and the greater amount of air traffic during the hours encompassing the N16 overpass times (Fig. 2b) compared to those around the N15 overpass times (Fig. 2a).

The reasons for this diurnal mismatch in contrail coverage and air traffic density are not obvious. It is unlikely that the satellite algorithm or sensor sensitivities are responsible given the similar diurnal variation from the surface and the results of the error analysis noted above. Other potential causes for reduced contrail observations

include a decrease in afternoon humidity or more obscuration by thick cirrus clouds. There are two different ways that relative humidity could change to cause the morning-afternoon difference in contrails: large-scale diurnal variations in the upper tropospheric humidity (UTH) and depletion of supersaturation in a given air mass by contrail formation and precipitation into lower layers. The average domain relative humidity (RH) between 200 and 300 hPa was computed for the morning and afternoon overpass times during January, April, July, and October 2001 from the hourly Rapid Update Cycle (RUC) numerical weather analysis dataset used by DUDA et al. (2005). The mean morning and afternoon values of RH are the same, 36%. Thus, variations in synoptic scale RH cannot account for the morning-afternoon decrease in contrail coverage and frequency.

The flight-layer drying effect by crystal sedimentation (e.g., FAHEY et al., 1999) would tend to support a morning maximum in contrail cover and would not be included in numerical weather analyses. When a layer of air has sufficient water vapor for contrail formation and spreading, part of the water vapor will be removed by the contrails. If the layer is rising, the relative humidity (RH) will increase as the day proceeds and the contrail should grow rapidly and possibly precipitate more large crystals because of the greater RH or the layer begins forming natural cirrus. If not permanently removed by precipitation, the water vapor will remain locked in the contrails until the layer sinks. At that point, contrails will no longer form in the layer anyway. With reduced humidity in the layer because of earlier flights, the contrails could be less likely to form and less likely to spread as much in the affected layer even if it is neither sinking or rising. Because air is rising and sinking at different locations throughout the day, this contrail "saturation" effect would only alter the contrail potential in areas of heavy air traffic where the layer ascent is minor. Also, in heavy air traffic, spreading contrails might also produce a non-uniform cirrus deck that can obscure contrails. This sedimentation explanation is only speculative at this point because no data are available for testing it and large-scale contrail models with fully interactive water vapor and microphysics have not been developed yet. However, upper tropospheric drying by contrails is a long-standing question that should be addressed.

The presence of more clouds, especially thick cirrus clouds, during the afternoon would tend to obscure contrails formed within, below, or even slightly above the clouds. A detailed study of the diurnal cycle of cirrus clouds is beyond the purview of this paper. However, some information about their impact can be gleaned from the surface observations of MINNIS et al. (1997), which provide data about obscuration from the surface. Their two indeterminate categories include obscuration of the flight level by clouds or haze and by cirrus, in par-

Table 4: Comparison of estimated USA contrail coverage (%).

Month	Current study 2001	Current study Diurnal correction	PALIKONDA et al. (1999) 1993–94	SAUSEN et al. (1998) Theoretical 1992
April	1.00	0.71	2.0	2.0
July	0.67	0.48	1.3	0.5
October	0.90	0.64	1.9	1.9
December	0.89	0.63	2.1	1.6 (Jan)

ticular. Averaging of those data for the overpass times indicates that both indeterminate categories were reported slightly more often during the morning than during the N16 overpass period. These results suggest that contrails were more likely to be observable during the afternoon from the surface, yet contrails were seen more frequently during the morning indicating that obscuration cannot explain the diurnal cycle in contrail frequency from the surface. While this is not an ideal dataset for evaluating obscuration of the view from the top, it suggests that, on average, there are fewer clouds below the contrail altitudes during the N16 times so that the contrast between the contrail and the background should be greatest during the afternoon. To fully explore this issue, it will be necessary to perform a more detailed analysis of average cirrus coverage over the domain during the course of the day.

5 Relative humidity effects

Two conditions are necessary for contrail formation: air traffic and suitable atmospheric conditions. The air traffic over the domain is relatively heavy with more than 4000 km of potential contrails (flights above 7 km) every day in a given 1° box (GARBER et al., 2005). Thus, the contrail coverage can be dominated by formation conditions. DUDA et al. (2005) estimated the frequency of potential contrail conditions over a similar domain using RUC model data. Figure 3 in DUDA et al. (2005) shows potential coverage results for September 2001 that are very similar to the afternoon contrail coverage in Figure 5. Similar correspondence was also found for November (not shown). Overall, the RUC-based potential contrail frequency during 2001 peaked during April at 30 % and dropped to a minimum of ~12 % during the summer months, nearly reaching a secondary peak in November followed by a decrease during December (see Figure 1 in DUDA et al., 2005). The sequence is very similar to the observed contrail variation in Table 1. The contrail coverage is considerably less than the potential because the contrails only form when the air-traffic coincides with the moisture and can only be detected when existing clouds do not obscure them. This consistency with contrail potential and the nearly identical morning-afternoon optical depths in Figure 8 support the validity of the retrievals.

Although the relative seasonal variations between 1993–94 and 2001 are nearly identical, Table 4 reveals that the contrail coverage is only half of that detected by PALIKONDA et al. (1999) from 1993–94 NOAA-11 and 12 AVHRR data and calculated by Sausen et al. (1998) using 1992 air traffic densities and multiple years of meteorological data. The differences are even greater if the daytime sampling is corrected for the absence of nighttime coverage. Using data from GARBER et al. (2005), it was determined that the daytime averages should be multiplied by 0.71 to estimate the impact of diminished air traffic at night. The diurnally corrected results are also listed in Table 4. If the overestimate indicated by the error analysis is correct, then the means should probably be decreased by an additional 40 %. This dramatic difference between the expected and observed linear contrail coverage is puzzling. Because the air traffic should have risen by more than 30 % or more between 1992 and 2001 (e.g., MINNIS et al., 2004), the contrail coverage also should have increased.

Part of the reduction may be due to overestimates in the NOAA-11 and NOAA-12 analyses, but decreased RH is also a likely reason. MINNIS et al. (2003) found a diminished frequency of persistent contrails over the USA during 1999 relative to 1993–94 that corresponded to a drop in UTH as indicated by the mean RH at 300 hPa from the National Center for Environmental Prediction (NCEP) reanalyses data. As seen in Figure 8, the UTH was 45.5 % during 1993–94 and decreased to 39.4 % during 2001, one of the lowest values during the 30-year period. Since RH is a crucial factor in the formation of contrails, a reduction in RH should result in reduction of contrail cover and frequency of occurrence. From correlations of mean cirrus cloudiness and UTH in areas without heavy air traffic, MINNIS et al. (2004) found that cirrus coverage decreases by an average of 0.4 % UTH. Thus, the cirrus amount would have diminished by ~2.5 % over the USA and, probably, the surrounding areas between 1993–94 and 2001 and would likely include a decrease in contrail coverage.

6 Comparisons with other results

The phasing of the observed seasonal cycles in contrail coverage in Table 1 differs from the theoretical results of SAUSEN et al. (1998) and PONATER et al. (2002),

but is consistent with the contrail frequency observations from surface observations (MINNIS et al., 2003). The seasonal range (200 %) in f_c is only half of that (400 %) observed from the surface and computed theoretically. This range difference decreases if only the N16 values are used.

The seasonal variation in OD is similar to that computed by PONATER et al. (2002) with a maximum during the summer. Additionally, the greater occurrence of optically thick contrails during summer (Table 2 and Figure 8) is consistent with the greater maximum contrail optical depth computed by PONATER et al. (2002). However, the theoretical winter minimum relative to the summer maximum is significantly less than the observations. On average, the observed ODs are twice the value of those computed theoretically and 2.5 times more than those found over Europe by MEYER et al. (2002). Part of the difference may be due to contrails forming at higher temperatures over this North American domain than over Europe (PONATER et al., 2002). Higher temperatures would increase the availability of more water vapor for ice particle growth over North America. The use of the same fixed contrail temperature over both locations could introduce an artificial difference if the North American contrails are actually warmer, on average, than those over Europe. Another source of discrepancies in the OD could be the differences in the contrail particle emissivity model and the particle sizes. The ice crystal diameter in (2.2) has a diameter of 20 μm compared to the 34 μm used by MEYER et al. (2002). Another possible source of the OD discrepancies could be different detection sensitivities between the NOAA-14 and N15/16 AVHRRs. Perhaps, the NOAA-14 analysis systematically misses contrails with larger ODs.

The CLRF values also are considerably larger than those derived by PONATER et al. (2002). Part of the difference is due to OD discrepancies. The remaining differences are likely a result of differences in the background temperatures and the diurnal cycle in contrail coverage that is not included here. NCLRF in Table 2 is $\sim 3 \text{ Wm}^{-2}$ greater than the nighttime value computed by MEYER et al. (2002). Given the differences in OD and the greater surface temperatures during the daytime, a larger difference would be expected. However, MEYER et al. (2002) used a model calculation assuming a clear land surface while the result here used the actual background radiances to estimate the amount of forcing. Since contrails often occur with cirrus clouds and even within cirrus clouds, the radiative forcing should be smaller than that for clear sky conditions.

The mean NCLRF is roughly equal to the normalized net radiative forcing computed by MINNIS et al. (1999) suggesting that the previous result is slightly too large. According to the results of MINNIS et al. (1999), the NCLRF should be approximately 1.5 times greater than

the net radiative forcing so that NCLRF in the previous study would be about 23 Wm^{-2} for the domain latitude band after accounting for the OD differences between the current and previous study. MINNIS et al. (1999) assumed random overlap between contrails and average cloud cover. The current results are probably lower because contrails occur more frequently with a cirrus background than the random overlap assumption. The background would affect both the longwave and shortwave fluxes, so it is not possible without an explicit evaluation of the shortwave impact to comment on the net radiative forcing for this dataset.

7 Concluding remarks

The results shown here confirm, for the most part, the relative seasonal variations in contrail coverage and optical depths. Over the domain, contrail coverage peaks during the winter and spring and bottoms out during the late summer. Contrail optical depth is greatest during summer, approximately 20 % larger than the winter minimum value. Uncertainties in the magnitudes of contrail coverage are large. The detailed error assessment indicates that the automated contrail detection method overestimates contrail coverage by 40 % from both satellites. Refinements in the algorithm are needed to reduce this error. The probability distributions and mean values of the contrail optical depths and normalized contrail radiative forcing are relatively robust and appear to be insensitive to the presence of falsely detected contrails. Their values are significantly larger than those found theoretically and from satellite analyses over Europe. Additional analyses are needed to help resolve some of the remaining large differences between the theoretical calculations and the observations. Until these discrepancies are understood, it will not be possible to determine conclusively if the current model estimates are sufficiently accurate for estimating contrail climate effects or whether additional improvements are needed. While the contrail longwave radiative forcing has been estimated empirically, this study has not addressed the net radiative forcing. The shortwave radiative forcing is more difficult to estimate because of the large anisotropy in the radiation field and the solar zenith angle dependence of the albedo. Estimation of the net forcing will be addressed in future research.

Additional discrepancies between the total contrail coverage found here and previous empirical and theoretical calculations can be explained to some extent by interannual variations in UTH which can have a large impact on contrail frequency and coverage. Whether it can explain the differences found here remains an open question that, perhaps, could be answered by examining the interannual variability in multi-year modelling results and deriving contrail coverage over the domain

for other years. A morning-afternoon diurnal cycle in contrail coverage that is not governed by air traffic was found. It is characterized by a decrease during the afternoon that is most significant during summer. The reason for this diurnal cycle is currently unknown. More detailed modelling and an evaluation of obscuring cirrus clouds are needed to better quantify why it occurs and to account for it in estimating contrail effects. The analysis of the diurnal cycle here was constrained by the lack of morning satellite data over the western portion of the domain. Future study of the diurnal and interannual variability of contrail coverage will require analyses of morning data taken in other years over the entire domain.

Acknowledgements

This research was supported by the NASA Pathfinder Program and the NASA Office of Earth Science Radiation Sciences Program. Many thanks to Don GARBER for supplying the air traffic figures and to the two anonymous reviewers who provided helpful comments.

References

- DUDA, D. P., P. MINNIS, L. NGUYEN, 2001: Estimates of cloud radiative forcing in contrail clusters using GOES imagery. – *J. Geophys. Res.*, **106**, 4927–4937.
- DUDA, D. P., P. MINNIS, P. K. COSTULIS, R. PALIKONDA, 2005: CONUS contrail frequency from RUC and flight track data. – *Meteorol. Z.* **14**, 537–548.
- GARBER, D. P., P. MINNIS, P. K. COSTULIS, 2005: A USA commercial flight track database for upper tropospheric aircraft emission studies. – *Meteorol. Z.* **14**, 445–452.
- FAHEY, D. W., U. SCHUMANN, S. ACKERMAN, P. ARTAXO, O. BOUCHER, M. Y. DANILIN, B. KÄRCHER; P. MINNIS, T. NAKAJIMA, O. B. TOON, 1999: Aviation-Produced Aerosols and Cloudiness. – Chapter 3 of IPCC Special Report: Aviation and the Global Atmosphere. – Cambridge University Press, 65–120 pp.
- MANNSTEIN, H., R. MEYER, P. WENDLING, 1999: Operational detection of contrails from NOAA AVHRR data. – *Int. J. Remote Sens.* **20**, 1641–1660.
- MEYER, R., H. MANNSTEIN, R. MEERKÖTTER, U. SCHUMANN, P. WENDLING, 2002: Regional radiative forcing by line-shaped contrails derived from satellite data. – *J. Geophys. Res.* **107**, [D10 10.1029/2001JD000426](https://doi.org/10.1029/2001JD000426).
- MINNIS, P., W. L. SMITH, Jr., 1998: Cloud and radiative fields derived from GOES-8 during SUCCESS and the ARM-UAV Spring 1996 Flight Series. – *Geophys. Res. Lett.* **25**, 1113–1116.
- MINNIS, P., Y. TAKANO, K.-N. LIOU, 1993: Inference of cirrus cloud properties using satellite-observed visible and infrared radiances, Part I: Parameterization of radiance fields. – *J. Atmos. Sci.* **50**, 1279–1304.
- MINNIS, P., J. K. AYERS, S. P. WEAVER, 1997: Contrail occurrence frequency over the U.S., April 1993 – April 1994. – NASA Reference Publication **1404**.
- MINNIS, P., D. P. GARBER, D. F. YOUNG, R. F. ARDUINI, Y. TAKANO, 1998a: Parameterization of reflectance and effective emittance for satellite remote sensing of cloud properties. – *J. Atmos. Sci.* **55**, 3313–3339.
- MINNIS, P., D. F. YOUNG, L. NGUYEN, D. P. GARBER, W. L. SMITH, JR., R. PALIKONDA, 1998b: Transformation of contrails into cirrus during SUCCESS. – *Geophys. Res. Lett.* **25**, 1157–1160.
- MINNIS, P., U. SCHUMANN, D. R. DOELLING, K. M. GIERENS, D. W. FAHEY, 1999: Global distribution of contrail radiative forcing. – *Geophys. Res. Lett.* **26**, 1853–1856.
- MINNIS, P., L. NGUYEN, D. P. DUDA, R. PALIKONDA, 2002: Spreading of isolated contrails during the 2001 air traffic shutdown. – 10th AMS Conf. Aviation, range, and Aerospace Meteorol., Portland, OR, May 13–16, 33–36.
- MINNIS, P. J. K. AYERS, M. L. NORDEEN, S. WEAVER, 2003: Contrail frequency over the United States from surface observations. – *J. Climate* **16**, 3447–3462.
- MINNIS, P., J. K. AYERS, R. PALIKONDA, D. PHAN, 2004: Contrails, cirrus trends, and climate. – *J. Climate* **17**, 1671–1685.
- MINNIS, P., R. PALIKONDA, B. J. WALTER, J. K. AYERS, H. MANNSTEIN, 2005: Contrail coverage over the North Pacific from AVHRR data. – *Meteorol. Z.* **14**, 515–523.
- PALIKONDA, R., P. MINNIS, D. R. DOELLING, P. W. HECK, D. P. DUDA, H. MANNSTEIN, U. SCHUMANN, 1999: Potential radiative impact of contrail coverage over continental USA estimated from AVHRR data. – Proc. AMS 10th Conf. Atmos. Rad., Madison, WI, June 28–July 2, 181–184.
- PONATER, M., S. MARQUART, R. SAUSEN, 2002: Contrails in a comprehensive global climate model: parameterisation and radiative forcing results. – *J. Geophys. Res.* **107**, [10.1029/2001JD000429](https://doi.org/10.1029/2001JD000429).
- SAUSEN, R., K. GIERENS, M. PONATER, M. U. SCHUMANN, 1998: A diagnostic study of the global coverage by contrails, part I, present day climate. – *Theor. Appl. Climatol.* **61**, 127–141.